Light absorption efficiencies of photosynthetic pigments: the dependence on spectral types of central stars

doi: 10.1017/S147355041400072X

Light absorption efficiencies of photosynthetic pigments: the dependence on spectral types of central stars

Yu Komatsu[1], Masayuki Umemura[1], Mitsuo Shoji[1], Megumi Kayanuma[2], Kazuhiro Yabana[1], and Kenji Shiraishi[3]

[1]Graduate School of Pure and Applied Sciences, University of Tsukuba
[2]Graduate School of Systems and Information Engineering, University of Tsukuba
[3]Graduate School of Engineering, Nagoya University

Abstract

For detecting life from reflection spectra on extrasolar planets, trace of photosynthesis is one of the indicators. However, it is not yet clear what kind of radiation environments are acceptable for photosynthesis. Light absorption in photosystems on the earth occurs using limited photosynthetic pigments such as chlorophylls (Chls) and bacteriochlorophylls (BChls). Efficiencies of light absorption for the pigments were evaluated by calculating the specific molecular absorption spectra at the high accuracy-quantum mechanical level. We used realistic stellar radiation spectra such as F, G, K, M type star to investigate the efficiencies. We found that the efficiencies are increased with the temperature of stars, from M to F star. Photosynthetic pigments have two types of absorption bands, the Q_y and Soret. In higher temperature stars like F star, contributions form the Soret region of the pigments are dominant for the efficiency. On the other hand, in lower temperature stars like M stars, the Q_y band is crucial. Therefore, differences on the absorption intensity and the wavelength between the Q_y and Soret band are the most important to characterize the photosynthetic pigments. Among photosynthetic pigments, Chls tend to be efficient in higher temperature stars, while BChls are efficient for M stars. Blueward of the 4000 Å break, the efficiencies of BChls are smaller than Chls in the higher temperature stars.

Introduction

Currently, more than 1800 extrasolar planets have already been confirmed since the first extrasolar planet was discovered (Mayor & Queloz 1995). In the series of searching for second earths, exoplanets in the habitable zone, where the planets can sustain liquid water, have been detected in succession (Anglada-Escudé *et al*. 2013; Broucki *et al*. 2013). The habitable zone is one requirement to guess whether a planet has life or not. Another index is to identify biosignatures or biomarkers, which are trace of life from reflection spectra of extrasolar planets. Spectral features which derive from photosynthetic activities can be biosignatures. The vegetation red edge is one of them (Seager *et al*. 2005, Kiang *et al*. 2007).

Nowadays, developments of quantum chemical calculations permit us to evaluate highly accurate absorption spectra for photosynthetic pigments. Photosystem is a very complicated system composed of protein complexes, and they contain many types of the pigments. By using theoretical approaches, each absorption feature of the specific pigment is easily calculated only assuming the molecular structure. In principle, there are possibilities to optimize a photosystem at the atomic level. Therefore, it is a great challenge to clarify the light absorption process in photosystems on exoplanet situations. For example, we can construct photosystems whose pigment arrangements and molecular structures are modified even though these complexes are difficult to be formed experimentally. It is beyond the scope of this paper, but these theoretical approaches will be very significant to predict novel photosystems.

The major photosynthetic pigments found in organisms on the earth are chlorophylls (Chls), bacteriochlorophylls (BChls) and carotenoids. While Chls are contained in oxygenic photosynthetic organisms

such as plants and cyanobacteria, BChls are major pigments in the anoxygenic photosynthetic organisms such as purple bacteria, green sulfur bacteria, halobacteria (Canfield et al. 2006; Olson 2006). One role of carotenoids is quenching excited species such as singlet oxygen in addition to the light harvesting function, but the main light harvesting pigments in photosystems are Chls and BChls.

In this paper, the absorption spectra of six photosynthetic pigments were calculated at a quantum chemical method of the density functional theory (DFT). We investigated four Chl compounds: Chl *a*, Chl *b*, Chl *d* and Chl *f* and two BChl compunds: BChl *a* and BChl *b*. Their absorption efficiencies were evaluated by using some stellar spectra from F to M type stars, and we investigated how the pigments which exist on the earth absorb light efficiently on the environments. It is noted that actual efficiencies in photosynthesis are largely affected by other important factors such as atmospheric composition, structures of canopy and leaf, however, as a first step, direct light absorption efficiencies for the photosynthetic pigments are investigated.

Methods

Quantum chemical calculations were performed for the six major photosynthetic pigments. First, full geometry optimizations were carried out at DFT level using the B3LYP functional (Becke 1988). 6-31G(d) basis sets were used for all atoms. The initial structures of Chl *a*, Chl *b*, BChl *a* and BChl *b* were taken from x ray structures from *Thermosynechococcus vulcanus* (Umena *et al.* 2011), *Pisum sativum* (Standfuss *et al.* 2005), *Rhodopseudomonas acidophila* (Papiz *et al.* 2003) and *Rhodopseudomonas viridis* (Lancaster & Michel 1999), respectively. The structures of Chl *d* and *f* were obtained by substituting the Chl *a* structure. All the optimized structures are shown in Figure **??**. Absorption spectra were calculated based on the time-dependent density functional theory (TDDFT) (Marques & Gross 2004). The solvent effect of methanol was considered by the polarizable continuum model (PCM) methodology (Miertus *et al.* 1981). Other theoretical conditions used were the same as the geometry optimization calculations. All the calculations were performed using the Gaussian 09 quantum chemistry program package (Frisch *et al.* 2009).

After obtaining the absorption spectra, we evaluated the absorption efficiency χ_{photon} as described below. χ_{photon} is calculated using the photon flux spectrum from star.

$$\chi_{photon} \equiv \frac{\int \epsilon(\lambda) n(\lambda) d\lambda}{\int n(\lambda) d\lambda} \tag{1}$$

where $\epsilon(\lambda)$ is the absorption strength of the pigment at wavelength λ, and $n(\lambda)$ is the number density of photon at λ of stellar spectrum. Calculated TDDFT absorption spectra were used for $\epsilon(\lambda)$ after a correction to minimize a constant theoretical error. For the efficiency calculation, photon and energy representations exist. We adopted the photon representation because it is more suitable for describing efficiency of the redox reactions in photosynthesis (Chen & Blankenship 2011). The spectra of the seven stars were used as $n(\lambda)$: HD128167 (F2V star), HD114710 (G0V low-activity star), HD206860 (G0V high-activity star), the Sun (G2V star), HD22049 (K2V star), AD Leo (M4.5V star) and GJ644 (M3Ve star). The fluxes for each star were obtained as they would be received at the top of the atmosphere of a planet in the habitable zone (the Sun: Wehrli 1985, AD Leo and GJ644: Segra *et al.* 2005, the others: Segra *et al.* 2003). The integration range is from 200 to 10,000 nm.

Results and Discussions

The DFT-optimized structures of the photosynthetic pigments are shown in Figure **??**. Calculated absorption spectra for the pigments are also shown in Figure **??**. Absorption bands are called the Q_y, the Q_x and Soret (or the B) in order of wavelength. Excited energies in the Soret region are quenched quickly to the Q_y energy level. Light energies are transferred to photosynthetic reaction centers where redox reactions take place. In the case of oxygenic photosynthesis, water molecules are oxidized to oxygen molecules in photosystem II. Absorption spectra are different depending on the pigment types. Generally, absorption of BChls are more red-shifted than those of Chls. Among Chls, Chl *d* and Chl *f* absorb longer wavelength radiation compared to normal Chls (Chl *a* and Chl *b*). The TDDFT calculated spectra were qualitatively reproduced the experimental spectra. However, there still remains differences between the theoretical and

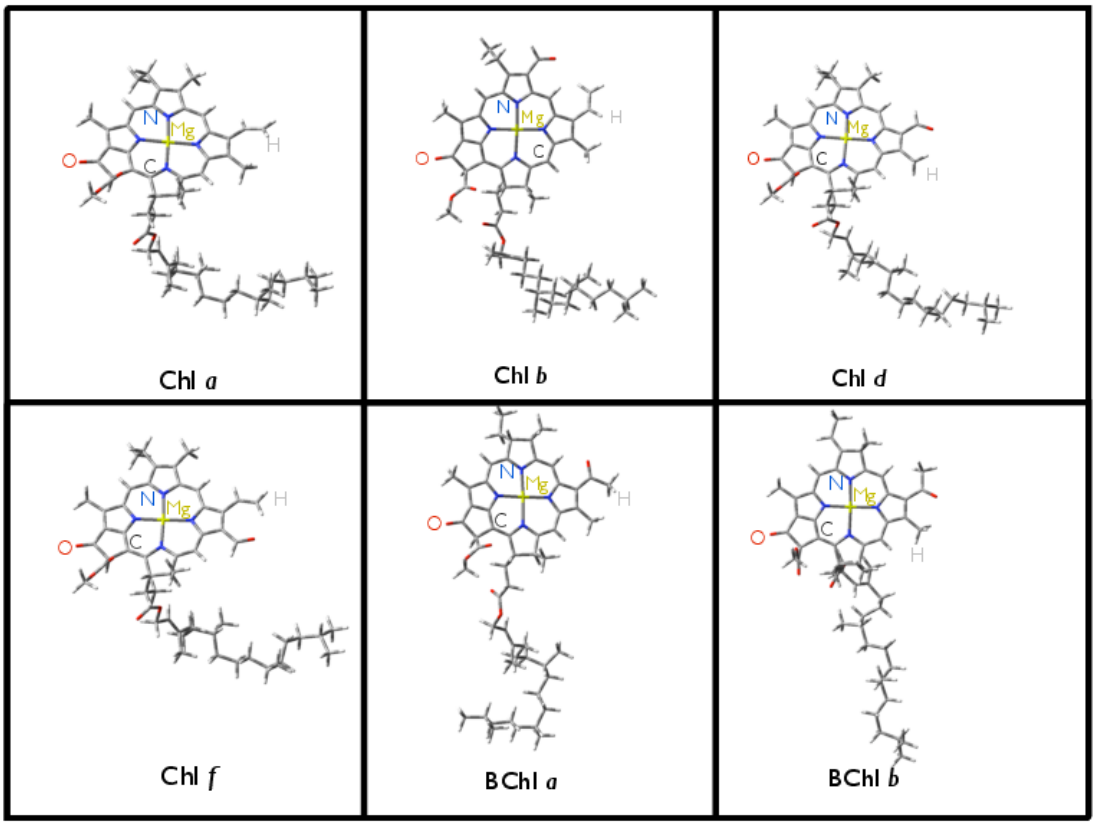

Figure 1: The structures of the photosynthetic pigment which are optimized by DFT calculations. Chl a, Chl b, Chl d, Chl f, BChl a and BChl b are shown.

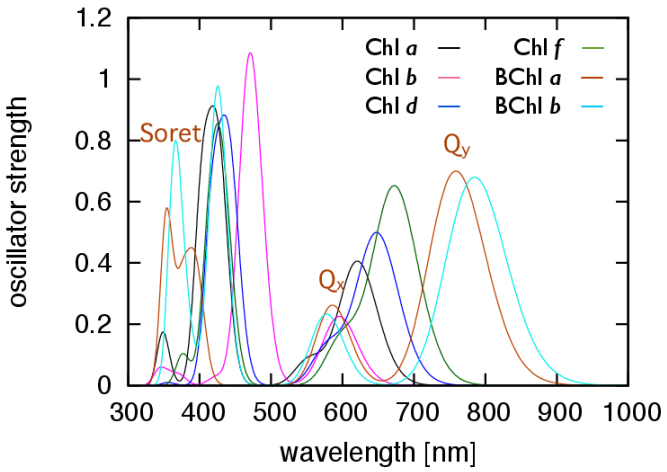

Figure 2: Calculated absorption spectra of pigments. The spectra of Chl a, Chl b, Chl d, Chl f, BChl a, BChl b are shown. These calculations were performed in methanol solvents. The positions of the main absorption bands in BChl a are labeled. These are called as the Q_y, the Q_x and Soret bands, in order of decreasing wavelength.

the experimental results (Table **??**). In order to minimize the systematic errors, the absorption wavelengths

Table 1: The calculated and the experimental wavelengths which exhibit the peaks in the Q_y and Soret bands. Those values in the Q_x bands are also shown only in BChls. The calibration lines in Figure **??** are shown as $y = 0.8521x + 129.99$ in the Q_y bands and $y = 0.5754x + 168.21$ in Soret bands, when x, y are the wavelengths from the TDDFT calculations and the experiments, respectively. In the case of the Q_x bands in the two BChls, $y = 2.9208x - 1132.8$.

	Chl *a*	Chl *b*	Chl *d*	Chl *f*	BChl *a*	BChl *b*
Q_y [nm] (calculation)	621.2	596.0	647.6	671.8	758.4	785.6
(experiment)	666.0	617.0	698.0	709.0	771.4	795.6
Q_x [nm] (calculation)	-	-	-	-	585.6	577.6
(experiment)	-	-	-	-	595.7	607.1
Soret [nm] (calculation)	418.4	470.6	434.0	425.4	353.6	366.4
(experiment)	433.0	422.0	429.5	407.0	364.8	373.2

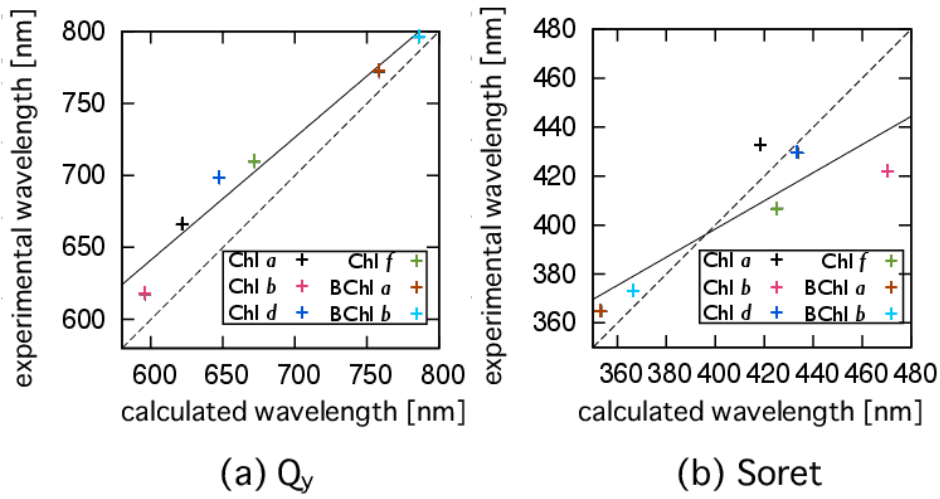

Figure 3: The calibration lines between the TDDFT and the experimental peaks of absorption bands in Table **??**. (a) The Q_y band. (b) Soret band.

at the Q_y and Soret peak tops were modified separately using calibration lines in Figure **??**. In the case of the Q_x, the same treatments are applied only in BChls, because the peaks of the Q_x bands are not often discerned clearly in Chls.

Figure **??** shows the energy correction for the absorption spectra of Chl *a*. Absorption energy corrections were also applied to the other pigments. For the correction of Soret band of Chl d, an average of absorption peak tops was used for the fitting. It is noted that experimental spectra of Chls were measured in methanol solvents (Chen & Blankenship 2011; Chen *et al*. 2005; Li *et al*. 2012; Chen *et al*. 2010), and those of BChls were measured in mixtures of methanol, acetonitrile, ethyl acetate and water solvents (Frigaaed *et al*. 1996). The peak wavelengths and the maximum absorption of each band after the calibrations are shown

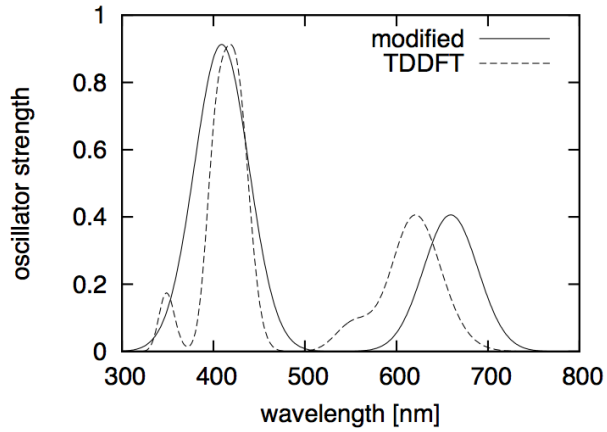

Figure 4: Absorption spectrum from the TDDFT calculation (solid line) and the modified spectrum (dashed line). The modified spectra were obtained from Figure **??**. The spectra of Chl *a* are shown here.

Table 2: The peak wavelengths and the maximum absorption of Soret and the Q_y bands in the six pigments. The values of the Q_x are shown only in BChls. The peak wavelength gaps between Soret and the Q_y bands are also revealed. The ratios of the integral of Soret band over wavelength to that of the Q_y are shown.

	Chl *a*	Chl *b*	Chl *d*	Chl *f*	BChl *a*	BChl *b*
peak wavelength [nm] in Soret	408.96	438.99	417.93	412.99	371.67	379.04
in Q_x	-	-	-	-	577.15	553.79
in Q_y	659.31	637.84	681.81	702.43	776.22	799.40
Q_y - Soret	250.35	198.85	263.88	289.44	404.55	420.36
maximum absorption in Soret	0.91	1.09	0.88	0.85	0.70	0.68
in Q_x	-	-	-	-	0.23	0.26
in Q_y	0.41	0.23	0.50	0.65	0.58	0.80
absorption ratio (Soret/Q_y)	2.25	4.82	1.77	1.31	0.83	1.18

in Table **??**. The two peak wavelengths of BChls are more separated than those of Chls. The ratios of the integral of Soret band over wavelength to that of the Q_y are shown, to investigate which band contributes to the absorption. When discussing the absorption efficiency in the next paragraph, these values works as indicators.

Using the corrected spectra, the absorption efficiencies were evaluated as shown in Figure **??**. The efficiencies were calculated for each absorption band of the pigments. From Figure **??**, we can see how these bands contribute to the efficiency. For example, if the ratio of the efficiency of the Q_y band to that of Soret is approaching to 1.0, the main contribution to the light absorption comes from the Q_y, not from Soret (see Figure **??** (ii)). The seven stellar spectra were used to calculate the efficiencies. In Figure **??**, the normalized stellar spectra and the calculated absorption spectra of the pigments are shown. As seen in Figure **??**, the fluxes in the 300 - 900 nm region decrease from F2V to M3Ve. Therefore, the efficiencies are expected to decrease as the star becomes cooler. Actually, the tendency is observed clearly with reference to the Sun values. For Chl *a*, efficiencies in F2V and M3Ve stars are calculated to be 1.478 and 0.068 times as much as that in the Sun. Because of the fluxes in the five high temperate stars like F, G and K stars are greater than those in the two M stars, the efficiencies in the two M stars are significantly smaller. In the Soret band regions in the five star, the large flux differences are observed according to the stellar types. Reflecting the differences, values of Soret vary largely than those in the Q_y. In comparison with these five high temperature stars, in the two M stars, the fluxes are almost negligible in the Soret band regions as shown in Figure **??**. It is understood that the ratio of the efficiency of the Q_y band to that of Soret is close to 1.0 as shown in Figure **??** (ii). Chl *b* is the exceptional case, because the ratio of absorption intensities in Soret to the Q_y band is larger (4.82 as shown in Table **??**). Therefore, the small ratio of the Q_y to Soret are observed for Chl *b* in M stars.

In the Q_x regions in BChls (Figure **??** (iii)), the large flux difference between the five high temperature stars and the late M stars is observed. The contribution of the Q_x can be seen, when the ratios of the efficiency of the Q_x to that of all the three bands are calculated. The ratios in the five stars are around 0.22, while those in the two M stars are 0.06 - 0.07, reflecting the great difference.

Absorption spectra of BChl *a* and *b* are broader compared to Chls. The gaps in the peak wavelengths are 198 - 290 nm and 404 - 421 nm in Chls and BChls, respectively, as shown in Table **??**. In the Q_y, BChls absorb longer wavelength radiation than Chls (Chls: 637 - 703 nm, BChls: 776 - 800 nm), and the radiation also decreases in the region as seen in Figure **??**. Therefore, as shown in Figure **??**, Chls are more efficient than BChls in the high temperature stars radiation, and vice versa, BChls are more efficient than Chls in lower temperature stars, M stars. In lower temperature stars like M stars, Soret bands do not contribute to the efficiencies anymore, and the Q_y bands mainly contribute to the light absorption. BChls become more efficient in M stars than Chls, reflecting the larger spectral overlaps in the Q_y band regions. On the other hand, shorter wavelength radiation are absorbed for BChls in the Soret band than for Chls. The maximum values of Soret bands are 408 - 439 nm in Chls, while those are 371 - 380 nm in BChls. In the five high temperature stars the fluxes also become small, blueward of the 4000 Å break, shorter than 400 nm. Therefore, BChls receive less photons, although Chls absorb more due to the large fluxes redward of the 4000 Å break. Actually, the efficiencies in BChls are lower than those in Chls in the five high temperature stars radiation. From F to M star, the efficiencies of the Soret region decrease definitely. In terms of receiving more photons in the Soret region, BChls have a disadvantage compared to Chls because of the small fluxes blueward of the 4000 Å break. Because BChls are considered to emerge on the earth prior to Chls, the organisms could become able to receive drastically more radiation at a certain time by using Chls.

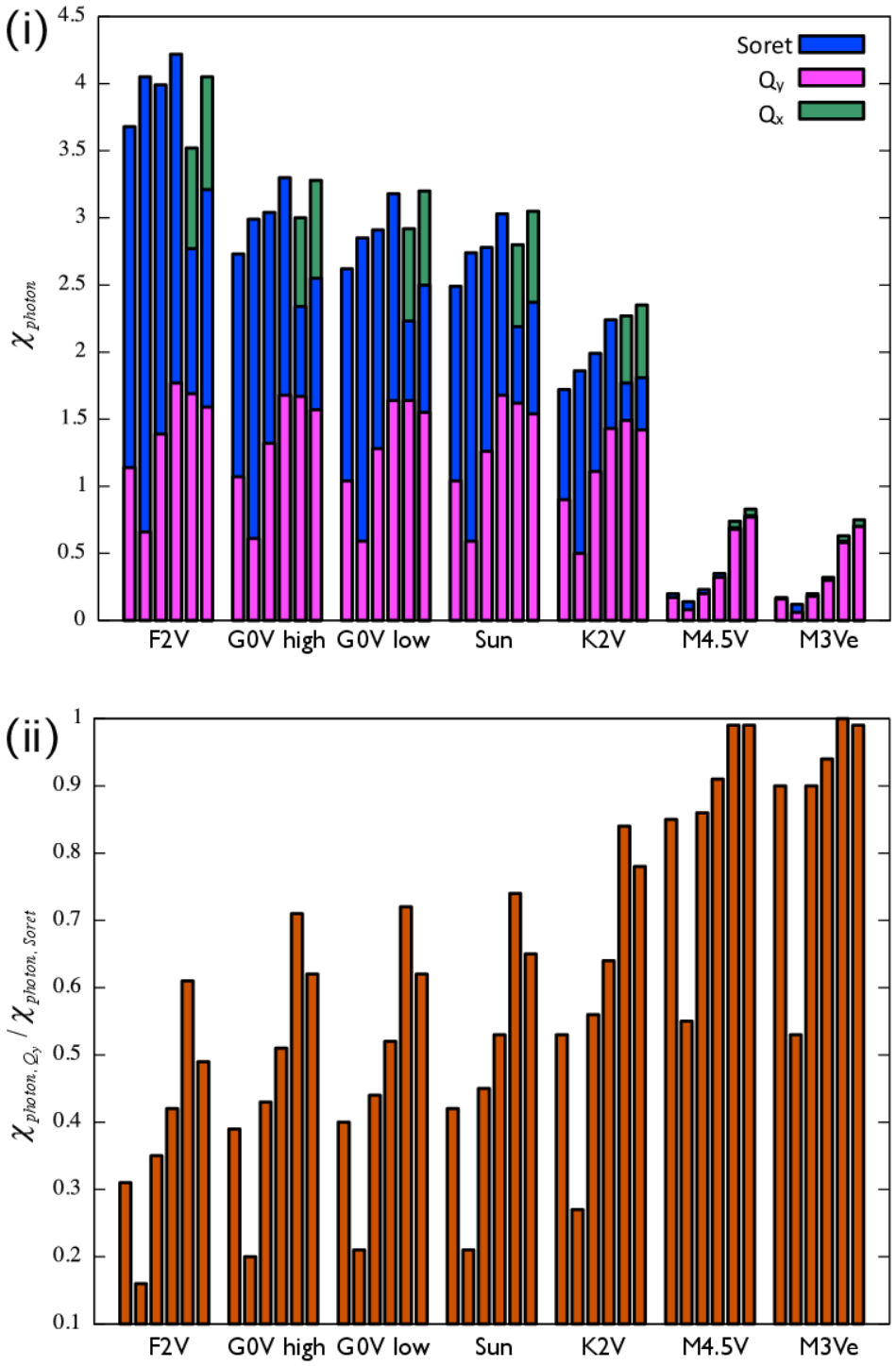

Figure 5: (i) The absorption efficiencies χ_{photon} (%). As stellar spectra, the seven spectra were used: F2V, G0V low-activity, G0V high-activity, K2V, M4.5V and M3Ve stars and the Sun. The six pigments are investigated: Chl a, Chl b, Chl d, Chl f, BChl a and BChl b in order left to right, in both (i) and (ii). The efficiencies are calculated using each band. In BChls, the efficiencies are also calculated from the Q_x. (ii) The ratio of the efficiency using the Q_y to that using Soret.

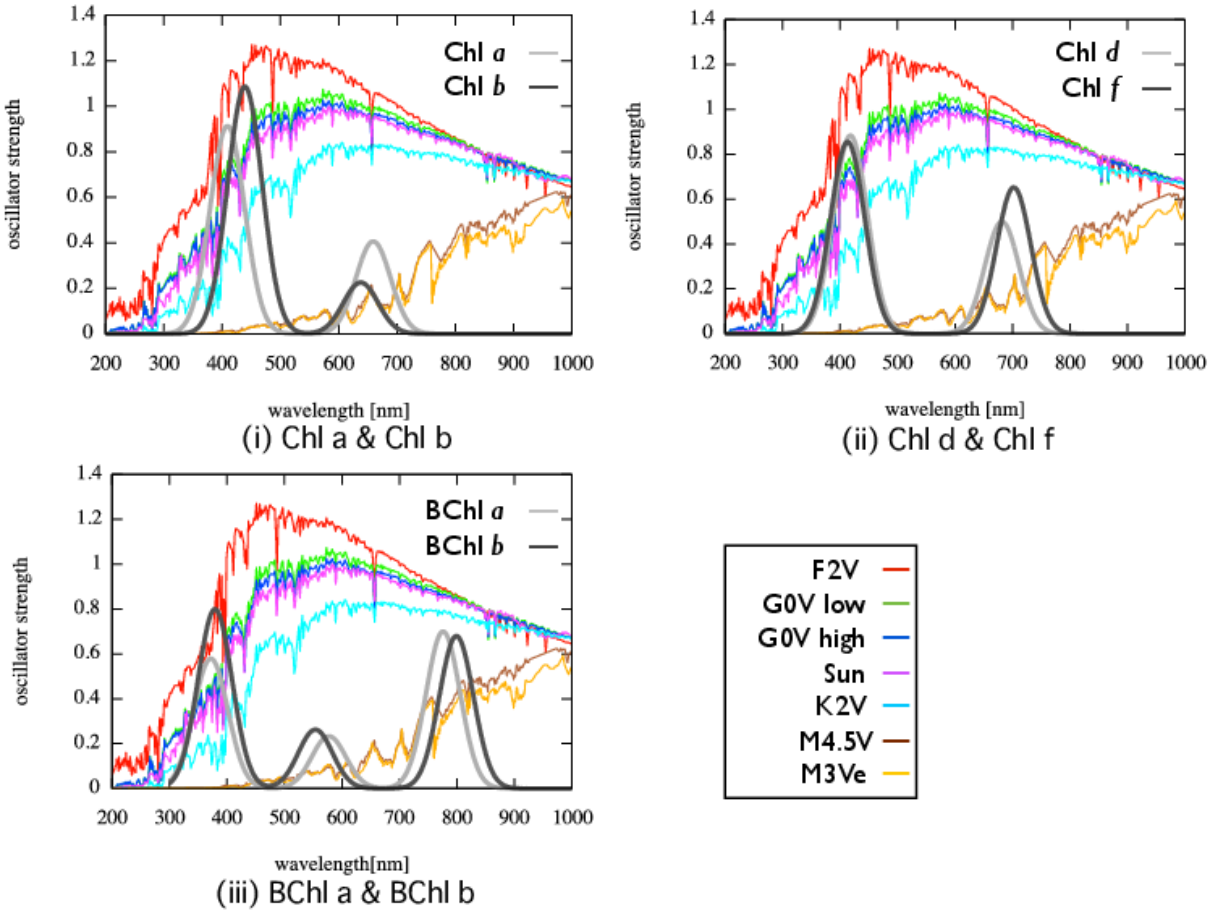

Figure 6: The calculated absorption spectra and the normalized stellar spectra. The absorption spectra of (i) Chl *a* & Chl *b*, (ii) Chl *d* & Chl *f* and (iii) BChl *a* & BChl *b* are shown. The vertical axis corresponds the oscillator strength. The seven stellar spectra are also shown: F2V, G0V low-activity, G0V high-activity, K2V, M4.5V and M3Ve stars and the Sun. The spectrum of the Sun is normalized so that the maximum value is 1.0. The other spectra are plotted as the integrated areas from 200 to 10,000 nm are equal to the area of the normalized spectrum of the Sun.

Conclusion

We have investigated how the photosynthetic organisms can absorb light from their host star and how the absorption efficiencies change depending on the photosynthetic pigments and star types. Six photosynthetic pigments were examined under real stellar radiation. Absorption spectra of the pigments were calculated by using a highly accurate quantum mechanical level and energy corrections were performed to minimize the theoretical error. Calculated efficiencies increased as higher the temperature of host star from M to F star. Contributions from the Q_y are almost saturated for higher temperature stars, K to F stars. In lower temperature stars like M stars, Soret bands do not contribute to the efficiencies anymore, and the Q_y bands mainly contribute to the light absorption. BChls become more efficient in M stars than Chls, due to the larger spectral overlaps in the Q_y band regions. On the other hand, contributions from Soret band increased, and the efficiencies of Chls are higher than BChls in the higher temperature stars, reflecting redward of the 4000 Å break.

Acknowledgements

This work was supported by Grant-in-Aid for JSPS Fellows (Y.K. 26·1303) from Japan Society for the Promotion of Science (JSPS).

Supplementary materials

For supplementary material for this article, please visit http://

References

[1] Anglada-Escudé, G., Tuomi, M., Gerlach, E., Barnes, R., Heller, R., Jenkins, J.S., Wende, S., Vogt, S.S., Butler, R.P., Reiners, A., Jones, H.R.A. 2013. arXiv:1306.6074.

[2] Becke, D.A. 1988, Phys, Rev. A 38, pp. 3098-3100.

[3] Borucki, W.J., Agol, E., Fressin, F., Kaltenegger, L., Rowe, J., Isaacson, H., Fischer, D., Batalha, N., Lissauer, J.J., Marcy, G.W., Fabrycky, D., Désert, J.-M., Bryson, S.T. Barclay, T., Bastien, F., Boss, A., Brugamyer, E., Buchhave, L.A., Burke, C., Caldwell, D.A., Carter, J., Charbonneau, D., Crepp, J.R., Christensen-Dalsgaard, J., Christiansen, J.L., Ciardi, D., Cochran, W.D., DeVore, E., Doyle, L., Dupree, A.K., Endl, M., Everett, M.E., Ford, E B., Fortney, J., Gautier III, T.N., Geary, J.C., Gould, A., Haas, M., Henze, C., Howard, A.W., Howell, S.B., Huber, D., Jenkins, J.M., Kjeldsen, H., Kolbl, R., Kolodziejczak, J., Latham, D.W., Lee, B.L., Lopez, E., Mullally, F., Orosz, J.A., Prsa, A., Quintana, E.V., Sanchis-Ojeda, R., Sasselov, D., Seader, S., Shporer, A., Steffen, J.H., Still, M., Tenenbaum, P., Thompson, S.E., Torres, G., Twicken, J.D., Welsh, W.F., Winn, J.N. 2013, Science 340, pp. 587-590.

[4] Canfield, D.E., Rosing, M.T., Bjerrum, C. 2006, Phil. Trans. R. Soc. B 361, pp.1819-1836.

[5] Chen, M., Blankenship, R.E. 2011, Trends in Plant Science 16, pp. 427-431.

[6] Chen, M., Eggink, L.L., Hoober, J.K., Larkum A.W.D. 2005, J. Amer. Chem. Soc. 127 pp. 2052-2053.

[7] Chen, M., Schliep, M., Willows, R.D., Cai, Z.-L., Neilan, B.A., Scheer, H. 2010, Science 329, pp. 1318-1319.

[8] Frigaard, N.-U., Larsen, K.L., Cox, R.P. 1996, FEMS Microbiology Ecology 20, pp. 69-77.

[9] Miertus, E., Scrocco, S., Tomasi, J. 1981, Chem. Phys. 55, pp. 117-129.

[10] Frisch, M.J., Trucks, G.W., Schlegel, H.B., Scuseria, G.E., Robb, M.A., Cheeseman, J.R., Scalmani, G., Barone, V., Mennucci, B., Petersson, G.A., Nakatsuji, H., Caricato, M., Li, X., Hratchian, H.P., Izmaylov, A.F., Bloino, J., Zheng, G., Sonnenberg, J.L., Hada, M., Ehara, M., Toyota, K., Fukuda,

R., Hasegawa, J., Ishida, M., Nakajima, T., Honda, Y., Kitao, O., Nakai, H., Vreven, T., Montgomery, Jr., J.A., Peralta, J.E., Ogliaro, F., Bearpark, M., Heyd, J.J., Brothers, E., Kudin, K.N., Staroverov, V.N., Kobayashi, R., Normand, J., Raghavachari, K., Rendell, A., Burant, J.C., Iyengar, S.S., Tomasi, J., Cossi, M., Rega, N., Millam, J.M., Klene, M., Knox, J.E., Cross, J.B., Bakken, V., Adamo, C., Jaramillo, J., Gomperts, R., Stratmann, R.E., Yazyev, O., Austin, A.J., Cammi, R., Pomelli, C., Ochterski, J.W., Martin, R.L., Morokuma, K., Zakrzewski, V.G., Voth, G.A., Salvador, P., Dannenberg, J.J., Dapprich, S., Daniels, A.D., Farkas, Ö., Foresman, J.B., Ortiz, J.V., Cioslowski, J., Fox, D.J. 2009, Gaussian 09, Revision A.01 , Wallingford CT

[11] Kiang, N.Y., Siefert, J., Govindjee, Blankenship, R.E. 2007, Astrobiology 7, pp. 222-251.

[12] Lancaster, C.R., Michel, H. 1999, J Mol Biol. 286, pp. 883-898.

[13] Li, Y., Scales, N., Blankenship, R.E., Willows, R.D., Chen, M. 2012, Biochim. Biophys. Acta 1817, pp. 1292-1298.

[14] Mayor, M., Queloz, D. 1995, Nature 378, pp. 355-359.

[15] Marques, M.A.L., Gross, E.K.U. 2004, Annual Review of Physical Chemistry 55, pp. 427-455.

[16] Olson, J.M. 2006, Photosynth. Res. 88, pp. 109-117.

[17] Papiz, M.Z., Prince, S.M., Howard, T., Cogdell, R.J., Isaacs, N.W. 2003, J Mol Biol. 326, pp. 1523-1538.

[18] Seager, S., Turner, E.L., Schafer, J. Ford, E.B. 2005, Astrobiology 5, pp. 372-390.

[19] Segura, A., Kasting, J.F., Meadows, V. Cohen, M. Scalo, J., Crisp, D., Butler, R.A.H., Tinetti, G. 2005, Astrobiology, 5, pp. 706-725.

[20] Segura, A., Krelove, K., Kasting, J.F., Sommerlatt, D., Meadows, V., Crisp, D., Cohen, M., Mlawer, E. 2003, Astrobiology, 3, pp. 689-708.

[21] Standfuss, J., Terwisscha van Scheltinga A.C., Lamborghini, M., Kühlbrandt W. 2005, EMBO J. 24, pp. 919-928.

[22] Umena, Y., Kawakami, K., Shen, J.R., Kamiya, N. 2011, Nature 473, pp. 55-60.

[23] Wehrli, C. 1985, 615, Physikalisch-Meteorologisches Observatorium + World Radiation Center (PMO/WRC) Davos Dorf.